NANO LETTERS

2007
Vol. 7, No. 6
1701−1705

Three-Layer Core/Shell Structure in Au–Pd Bimetallic Nanoparticles

D. Ferrer,[†] A. Torres-Castro,[†] X. Gao,[†] S. Sepúlveda-Guzmán,[†] U. Ortiz-Méndez,[‡] and M. José-Yacamán*[,†,§]

Department of Chemical Engineering, The University of Texas at Austin, 1 University Station, MS C0400, Austin, Texas 78712, FIME, Universidad Autónoma de Nuevo León, A.P. 076 suc. "F", Cd. Universitaria C.P., San Nicolás de los Garza, N.L., 66450, México, and Texas Materials Institute, The University of Texas at Austin, Austin, Texas 78712

Received March 24, 2007; Revised Manuscript Received April 28, 2007

ABSTRACT

This paper describes the internal structure of Au–Pd nanoparticles exhibiting newly discovered three-layer core/shell morphology, which is composed of an evenly alloyed inner core, an Au-rich intermediate layer, and a Pd-rich outer shell. By exploitation of spatially resolved imaging and spectroscopic and diffraction modes of transmission electron microscopy (TEM), insights were gained on the composition of each one of the observed three layers, indicating a significant extent of intimate alloy among the monometallic elements.

Bimetallic nanoclusters attract great interest due to their unique catalytic, electronic, and optical properties different from those of the corresponding monometallic components.[1−5] It is well-known that adding a second metallic component enhances the activity, selectivity, and stability of pure metal catalysts.[6,7] This behavior may originate from an ensemble or a ligand effect.[1] The properties of bimetallic nanoparticles can vary dramatically not only with size, as happens in monometallic nanoclusters, but also with chemical composition. Controlling their structure and chemical ordering can be the starting point to prepare the building blocks for specifically tailored cluster-assembled materials.[3,4] In many cases bimetallic systems display a core/shell structure, where a thin shell of metal B surrounds a core of metal A. The B overlayer is usually strained and, thus, can present prominent catalytic properties.[8] Core/shell colloids with a strained metal shell attain widespread use in various applications that include plasmonics, biological sensing, and catalysis, which places them on the frontier of advanced materials chemistry.[9−12]

One of the most interesting systems in catalysis research is Au−Pd bimetallic catalysts, which is miscible at any ratio as can be seen from their phase diagram.[13] Au−Pd bimetallic nanoclusters are employed for the direct synthesis of hydrogen peroxide from H_2 and O_2, for hydrodesulfurization of thiophene, and the oxidation of alcohols to aldehydes.[14,15] They are excellent catalysts of trichloroethene, achieving a higher activity than pure palladium dispersions, which make of them effective agents for the remediation of various inorganic and organic groundwater contaminants.[16] Due to the wide applications of these Au−Pd catalysts, it is of great interest to study the structure of these bimetallic colloids.

The preparation methods of gold−palladium bimetallic can be divided into two categories: successive and simultaneous reduction.[3,4] The latter one involves the presence of metallic precursors in the same reaction system. The successive reduction includes the consecutive addition of metallic precursors in the batch reactor. Under some conditions, the simultaneous methods produce Au*core*−Pd*shell* structured particles.[1,5] On the other hand, the successive reduction of the precursors yields cluster-in-cluster structure[1,10] or mixtures of monometallic components, although core−shell structures have also been observed.[17,18] This uncertain situation arises from the complex steps of metal ion reduction, clustering, dynamical dissolution, and displacement involved in the actual formation process of nanoparticles.[19−21] Detailed internal structural characterization is a prerequisite for understanding nanoparticles formation process and its relation to potential practical applications.

The chemical and physical properties of bimetallic nanoparticles exhibiting core/shell structure strongly depend on whether the two monometallic elements are chemically segregated or intimately alloyed.[22] These materials can be grown by different microscopic mechanisms, either involving shell-by-shell growth on preexisting smaller cluster or comprising a structural transformation of the clusters.[23] Optical methods are commonly used to elucidate the monometallic elements distribution on bimetallic nanoparticles.

* Corresponding author. yacaman@che.utexas.edu.
[†] Department of Chemical Engineering, The University of Texas at Austin.
[‡] FIME, Universidad Autónoma de Nuevo León.
[§] Texas Materials Institute, The University of Texas at Austin.

10.1021/nl070694a CCC: $37.00
Published on Web 05/11/2007

However, optical measurements provide average information that may not reflect the heterogeneous nature of core/shell systems. The poorly understood growth mechanism of core/shell systems remains as a puzzling issue to be solved. A very interesting case was reported by Rodriguez−Gonzalez et al.[24] who found that in the case of Ag/Au when synthesized by successive reduction a multishell structure is produced.

This work aims at clarifying the formation process of the core−shell structure in bimetallic nanoparticles. Our approach consists in synthesizing polymer-protected Au−Pd nanoparticles by means of the polyol method. A core/shell structure was confirmed in gold−palladium colloids, obtained by successive reduction of their corresponding metallic salts. By taking advantage of high-resolution transmission electron microscopy (HRTEM), scanning TEM (STEM), energy-filtering TEM (EFTEM), and convergent-beam electron diffraction (CBED), we determined the influence of nanoparticles size on the chemical segregation of monometallic elements that form separate domains of gold and palladium. An alternative method of nanostructure determination is also described here, based on STEM and X-ray energy dispersive spectroscopy (XEDS). The STEM−XEDS technique allows detecting variations in chemical composition down to atomic level, so it is ideally suited for composition analysis of the internal structures of nanosized particles. We demonstrate that above a critical size Au−Pd nanoparticles exhibit a complex core/shell structure, in which alternate layers of Au atoms and Pd atoms, form three-layer morphology. These findings lead to elucidating the mechanisms governing the growth of core/shell bimetallic nanoparticles.

The colloidal dispersions of the Au−Pd bimetallic clusters, stabilized by polymers, were fabricated by successive alcoholic reduction of their constituent metal ions. Solutions of 0.1 M tetrachloroauric acid ($HAuCl_4$) and 0.05 M palladium chloride ($PdCl_2$) were prepared by dissolving the corresponding crystalline material in deionized water. The protective agent poly(*N*-vinyl-2-pyrrolidone) (PVP, 0.4 g, 3.6 mmol of monomeric units) and the $PdCl_2$ (2 mL, 1×10^{-5} mol) were then mixed in ethylene glycol. The mixed solutions were stirred and heated to refluxing at 140 °C under air. After a sudden change was noticed in the color of the solution from yellow to brown (indicating the reduction of Pd), the aqueous solution of $HAuCl_4$ (1 mL, 1×10^{-5} moles) was added and subsequently reduced. This mixture was finally refluxed again at 140 °C for 3 h under air. The total amount of both metals was always kept as 2×10^{-5} mol in 50 mL of the mixed solution. Nanoparticles with different compositions of gold and palladium, namely, AuPd, $Au_{0.75}Pd_{0.25}$, and $Au_{0.25}Pd_{0.75}$, and monometallic nanoparticles of Au and Pd were fabricated by the described method.

High-resolution and scanning TEM images and CBED were acquired using a JEOL 2010F (200 kV) transmission electron microscope equipped with a field emission gun and an ultra-high-resolution observation system. This instrument includes a scanning image device to operate as STEM from TEM in a serial manner. It also possesses several atom level probes connected to Oxford INCA X-ray energy dispersive spectrometer (EDS) and Gatan 2D digital-parallel acquisition

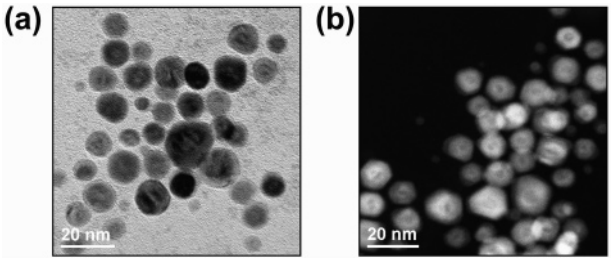

Figure 1. Low magnification transmission electron microscopy images of Au−Pd nanoparticles obtained by successive reduction of monometallic ions. Three alternate layers can be uniformly observed by high-resolution- (a) and scanning- (b) TEM images.

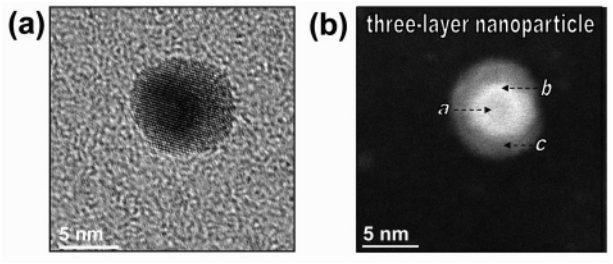

Figure 2. Detailed structure of Au−Pd nanoparticles at high magnification. The high-resolution- (a) and scanning- (b) TEM images confirm the presence of three different layers in the domains of the core/shell structure for typical single nanoparticles.

software. For EFTEM mappings and STEM−EDS line scanning, a FEI Tecnai F-20 field emission high-resolution transmission electron microscope (200 kV) was employed. This instrument has a Schottky type field emission source and it was operated at 200 kV as well. The point and line resolution are 0.24 and 0.10 nm, respectively. The equipped STEM−EDS system enables elemental analysis in the nanometer order. HRTEM images were obtained at the optimum Scherzer defocus for both instruments. In the case of STEM images, the HAADF detector integrated the signal over a large solid angle ranging from 60 to 150 mrad.

The synthesized samples were cleaned with acetone and ethanol to eliminate the residues of the protective and reducing agents. A 20 μL aliquot was then placed in a TEM grid of copper 01822-F PELCO, corresponding to ultrathin carbon, 400 mesh, with a grid hole size of 42 μm, backed on Formvar film. The backing film was removed before the addition of the nanoparticles aliquot. Conventional bright field and high angle annular dark field (HAADF) images for nanoparticles with composition AuPd are shown in Figure 1a and Figure 1b, respectively. Individual particles are displayed in Figure 2a and Figure 2b. It is possible to distinguish the presence of core/shell structure in Figure 2a, in which the core shows a dark spot in the center. However, the HAADF image in Figure 2b contains more information. We can clearly see three distinct regions on the image: the inner core at the center as a dark region marked with *a*, then a second intermediate region surrounding this core marked *b*, and an outer shell designated *c*. The shape of this particle determined by conventional dark field methods corresponds to truncated octahedron, which has (111) and (100) facets. The variations on the HAADF contrast cannot be explained

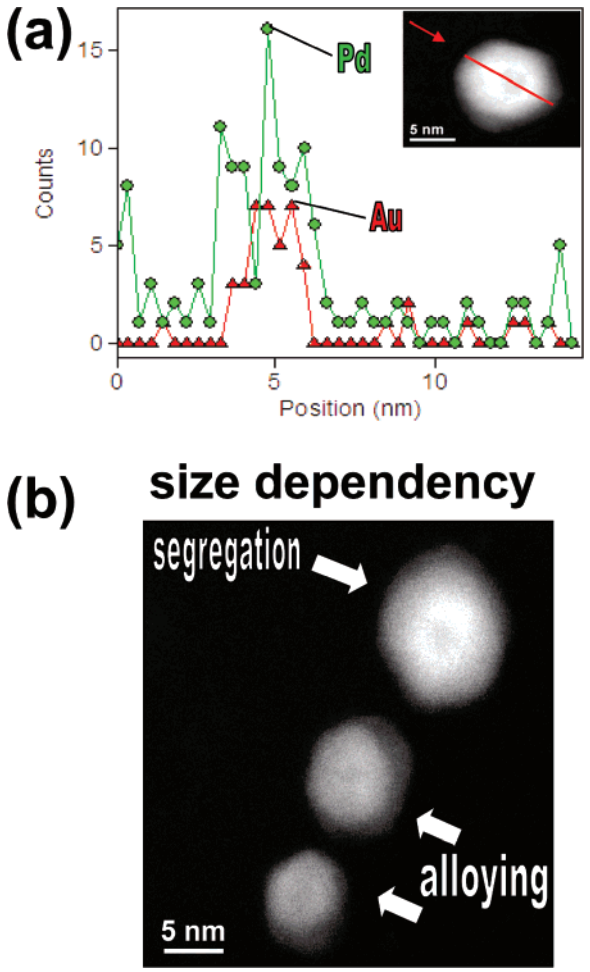

Figure 3. (a) Characterization of Au and Pd elemental distribution across the nanoparticle by STEM-XDS line-scanning technique. Inset shows analyzed area and the direction of analysis. (b) STEM-image revealing the influence of nanoparticles diameter on elemental segregation and alloying.

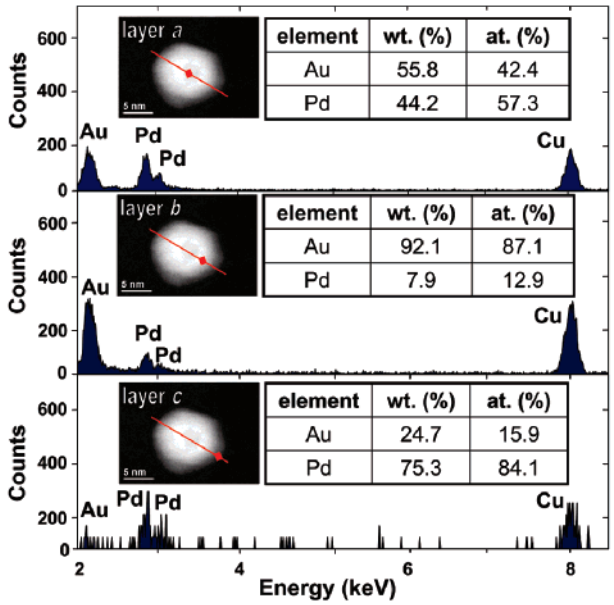

Figure 4. Quantitative elemental composition of layers *a* , *b* and *c*.

on the basis of thickness changes. Therefore, most important contributions should originate from compositional variations, revealed by the difference in atomic number (Z) that exists among gold and palladium. The HAADF intensity is considered to be proportional to $Z^{1.7}$.[25]

The distribution of the elements in the nanoparticles was assessed by using the line scanning analysis in the STEM−EDS mode (Figure 3a). This result revealed that Pd concentration peaks in the inner core and near the edges of the nanoparticles. On the other hand, the intermediate layers signaled Au and Pd peaks. It can be appreciated that the elemental signals are not symmetrical in the nanoparticles. However, these peaks corroborate the presence of layers with different compositions in the nanoparticles. It was also found that the three-layer core/shell structure in Au−Pd nanoparticles possess a diameter dependency (Figure 3b). The three-layer contrast does not appear for particles smaller than ∼5 nm, in which only two clear layers are observed. This was clarified by obtaining a STEM−EDS spectrum of nanoparticles below and above the critical diameter of 5 nm. Small nanoparticles show an alloyed structure among the inner core and the intermediate layer and a weak outer shell. In large nanoparticles Pd tends to situate on the periphery, whereas the Au locates in the center. A more quantitative analysis was performed in order to analyze the three layers observed in nanoparticles with diameter larger than 5 nm (Figure 4). This spectroscopic analysis showed that layer *a* has a uniformly alloyed composition of gold and palladium. The intermediate layer *b* is rich in gold, and this is consistent with the fact that shows the brightest region of the nanoparticle. The most external layer *c* has a large content of Pd, and this might explain the lower level of contrast observed. It is very interesting to note that neither the core nor the shell is composed of a single element, revealing elemental alloying events in the three detected layers. This is in contrast with the most accepted view.[26−28]

Additional information might be obtained by energy-filtering TEM (Figure 5a). This analytical tool allows chemical-sensitive imaging using ionization-loss electron energy, filtering the corresponding peak of the spectrum to produce an image. It can be appreciated that Au signal situates homogenously in the nanoparticles, from the inner core to the periphery, whereas the Pd preferentially locates in the inner core and periphery only. The reason of this distribution might be attributed to the differences in ionization potential that gold (9.2 eV) and palladium (8.3 eV) have. The gold has a larger affinity to gain electrons to reach the zero-valent state. Meanwhile the Pd has a smaller potential of reduction, and this could be the reason behind the faster formation of Au intermediate layers. However, considerable amounts of Pd situate in the inner center, which seems to be alloyed with gold. A note of caution should be made before straightforward analysis of the images. The gold peak is not easy to observe, and noise on the image can affect the profile. The image in Figure 4a only indicates that Pd mainly locates in the center and edges of the nanoparticle.

We also performed ultraviolet−visible (UV−vis) absorption studies of the nanoparticles for different compositions

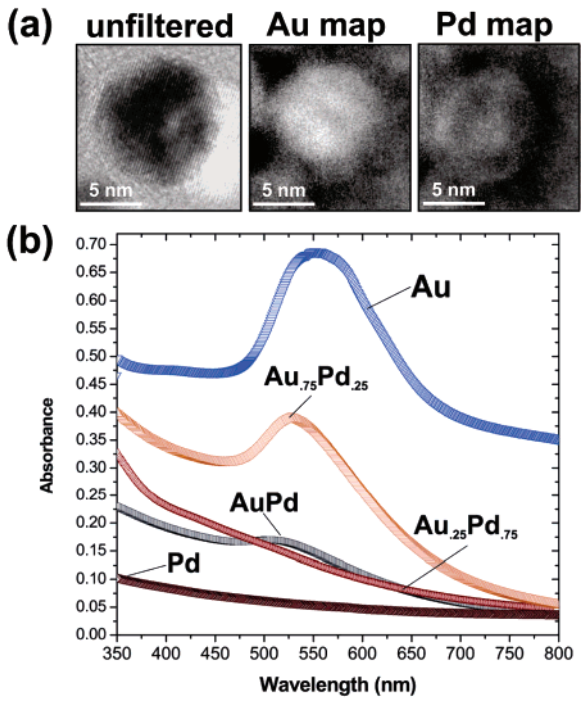

Figure 5. (a) Energy filtering images of Au−Pd nanoparticles. The map of gold clearly shows that the intermediate regions of the nanoparticle are rich in gold. On the other hand the external shell and inner-core contain signals of palladium. (b) The UV−vis absorption spectrum of the studied bimetallic nanoparticles shows the influence of the composition on the position of surface plasmon resonance peak.

as shown in the spectrum of Figure 5b. It can be observed that a very pronounced gold characteristic peak is obtained. Nevertheless, by increasing the concentration of palladium the intensity of the surface plasmon resonance peak of gold fades away. This is the spectroscopic evidence of the presence of Pd in the periphery of the nanoparticles. Another useful technique to assess the internal structure of nanoparticles is HRTEM. An image of an AuPd nanoparticle is shown in Figure 6. One immediate finding is that the crystal structure of the nanoparticle is face-centered cubic, and the morphology delineates a nicely shaped truncated octahedron. As can be seen in Figure 6, the edges of the particle are not smooth, forming instead a "zigzag" structure at the periphery due to atomic steps. The measurements of the lattice fringes showed different magnitudes in the three layers observed in the nanoparticles. The inner core (designated *a*) and external (designated *c*) layers have values of lattice spacing of 0.225 and 0.227 nm, respectively. On the other hand the intermediate region (designated *b*) presented a lattice spacing of 0.239 nm. A very interesting fact is that no Moiré fringes were observed in this HRTEM image. This suggests that there are no misorientations among the layers identified in the nanostructure. A model is proposed for the formation of the three-layer structure in Figure 7b. Our synthesis is based on the successive reduction of Pd and Au colloids. The formation of the three-layer structure includes the early reduction of Pd in the presence of PVP. Once the palladium reaches the zerovalent state, Au is introduced to the medium, to envelope the first coagulating clusters. However, the rest

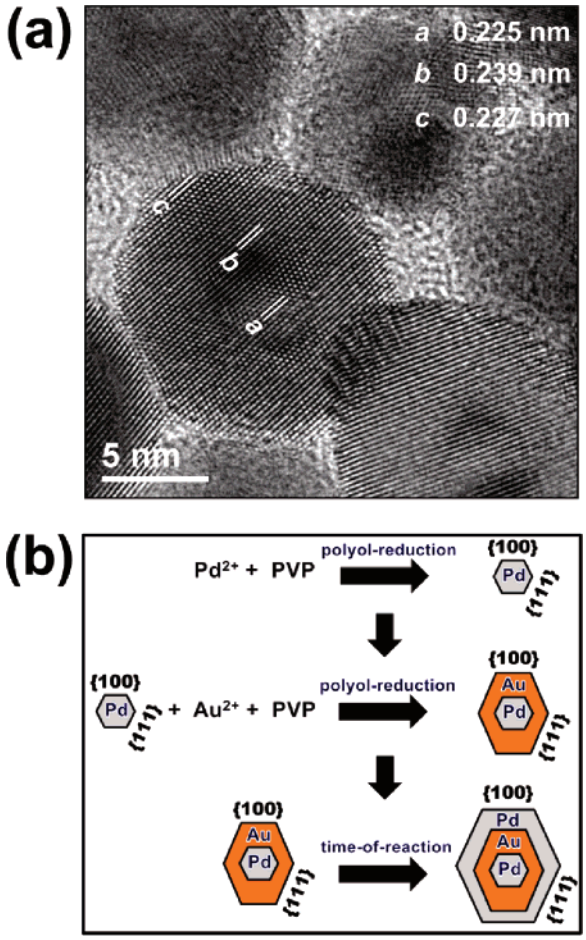

Figure 6. High-resolution TEM image displaying the lattice fringes of the Au−Pd nanoparticle (a). Model proposed for the formation of three-layer core/shell structure (b).

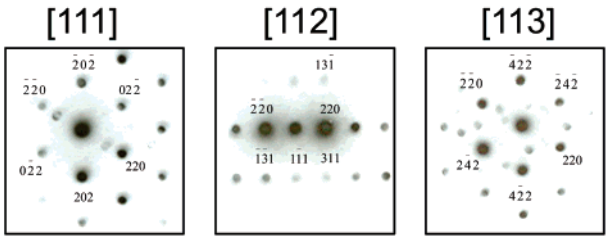

Figure 7. Diffraction patterns of AuPd nanoparticle for different directions.

of the ions in the solution grow in an epitaxial fashion that enables the formation of external layer of palladium enveloping the intermediate gold and the first reduced Pd clusters. Electron diffraction patterns collected from single nanoparticles are shown in Figure 7. We obtained nanodiffraction patterns of individual particles by concentrating the beam while still keeping it parallel, which enabled us to identify the crystalline system, precisely measure the lattice parameters and visualize true 3D symmetry of the atomic arrangement. The patterns were indexed, corresponding to the ⟨111⟩, ⟨112⟩, and ⟨113⟩ directions, evidencing the presence of single crystalline nanoparticles.

As previously stated, we determined that the nanoparticles with diameters below 5 nm present alloying events (Figure

3b). On the other hand, larger nanoparticles exhibit evidence of elemental segregation, leading to core/shell structure. Our results demonstrate that core/shell structure is not simple but fairly complex, containing three domains with different compositions. The inner core, containing an even mixture of Pd and Au, the intermediate layer corresponding to Au-rich composition, and a third (surface) layer with a Pd-rich alloy. The three-shell structure was theoretically predicted by Baletto et al.[23,29] However, spatially resolved details of an experimentally obtained three-layer structure are reported in this work for the first time. All of our results point to the fact that the external surface is rich in palladium. From a thermodynamic point of view, the separation of phases in a binary nanoparticle has been discussed by Shirinyan and Wautelet.[30,31] These authors show that the phase diagram of a nanoparticle is size dependent and is described by a solid−solid first-order phase transition. A two-phase separation taking place in the nanoparticle involves the shifting of the equilibrium phase diagram, compared with the bulk material. A chart of temperature versus concentration develops a cusp which is deeper for decreasing sizes.[30] The consequence of this is the formation of two equilibrium concentrations. This might explain the phase separation of the core/shell structure observed in Au−Pd nanoparticles. Further theoretical calculations predict that phase separation occurs only above a critical size.[30−32] This is in agreement with our TEM observations. The formation conditions of core/shell structure strongly depend on the temperature and initial composition. Nevertheless, it is clear that many topics should be clarified to completely understand the phase transitions in the nanosystems.

We have found that in the case of Au−Pd nanoparticles the successive reduction of the monometallic elements forms a three-layer structure. It was also determined that particle size plays a key role in the occurrence of intimate alloy or chemical segregation. Particles with diameters larger than 5 nm display three well-defined domains with presence of alloying events. Our results confirmed the early theoretical prediction of three-layer onion-like[24,29] structures in bimetallic nanoparticles. It is still intriguing to determine whether the three-layer structure is independent of the species composition. This newly reported three-layer structure should be very important to understand the catalytic activity of Au/Pd nanoparticles. It is very interesting that nanostructured Au/Pd does not show the same phase diagram as the bulk alloy. Comprehensive theories of phase diagrams at nanoscale reveal that phase diagrams become more complex as the size is reduced.[30,31] The details of the shift of the equilibrium phases with the size are related to the additional energy produced by the nanoparticle surfaces. An additional factor to consider could be a depletion effect,[32] which promotes a three-layer structure.

Acknowledgment. The authors thank the Center for Nano and Molecular Science and Technology, the Texas Materials Institute, and the International Center for Nanotechnology and Advanced Materials in The University of Texas at Austin. We also thank the support from the Welch Foundation and the NSF Grant DMR-0602587: "Alloys at the Nanoscale: The case of Nanoparticles".

References

(1) Toshima, N.; Yonezawa, T. *New J. Chem.* **1998**, 1179.
(2) Garcia-Gutierrez, D. I.; Gutierrez-Wing, C.; Miki-Yoshida, M.; Jose-Yacaman, M. *Appl. Phys. A-Mat. Sci. & Proc.* **2004**, *79*, 481.
(3) Garcia-Gutierrez, D. I.; Gutierrez-Wing, C. E.; Giovanetti, L.; Ramallo-Lopez, J. M.; Requejo, F. G.; Jose-Yacaman, M. *J. Phys. Chem. B* **2005**, *109*, 3813.
(4) Lee, A. F.; Baddeley, J.; Hardacre, C.; Ormerod, R. M.; Lambert, R. *J. Phys. Chem.* **1995**, *99*, 6096.
(5) Harada, M.; Asakura, K.; Toshima, N. *J. Phys. Chem.* **1993**, *97*, 5103.
(6) Xiang, Y.; Wu, X.; Liu, D.; Jiang, X.; Chu, X.; Li, Z.; Ma, L.; Zhou, W.; Xie, S. *Nano. Lett*. **2006**, *6*, 2290.
(7) Sastry, M.; Swami, A.; Mandal, S.; Selvakannan, P. R. *J. Mater. Chem*. **2005**, *15*, 3161.
(8) Gaikwad, A. V.; Verschuren, P.; Eiser, E.; Rothenberg, G. *J. Phys. Chem. B* **2006**, *110*, 17437.
(9) Cheng, D.; Wang, W.; Huang, S. *J. Phys. Chem. B* **2006**, *110*, 16193.
(10) Toshima, N.; Harada, M.; Yamazaki, Y.; Asakurat, K. *J. Phys. Chem.* **1992**, *96*, 9927.
(11) Baletto, F.; Mottet, C.; Ferrando, R. *Surf. Sci*. **2000**, *446*, 31.
(12) Nattamai, B. M.; Bhuvanesh, S. P.; Schaak, R. E. *J. Am. Chem. Soc*. **2005**, *127*, 7326.
(13) Phase Diagrams, 2nd ed.; ASM International: Materials Park, OH, **1992**; Vol. 1.
(14) Mejia-Rosales, S. J.; Fernandez-Navarro, C.; Perez-Tijerina, E.; Montejano-Carrizales, J. M.; Jose-Yacaman, M. *J. Phys. Chem. B* **2006**, *110*, 12884.
(15) Grzelczak, M.; Perez-Juste, J.; Rodrıguez-Gonzalez, B.; Liz-Marzan, M. *J. Mater. Chem*. **2006**, *16*, 3946.
(16) Nutt, M.; Hughes, J.; Wong, M. *Environ. Sci. Technol*. **2005**, *39*, 1346.
(17) Kim, Y.-G.; Garcia-Martinez, J. C.; Crooks, R. M. *Langmuir* **2005**, *21*, 5485.
(18) Kan, C.; Cai, W.; Li, C.; Zhang, L.; Hofmeister, H. *J. Phys. D Appl. Phys.* **2003**, *36*, 1609.
(19) Wu, M.-L.; Chen, D.-H.; Huang, T.-C. *Langmuir* **2001**, *17*, 3877.
(20) Mizukoshi, Y.; Fujimoto, T.; Nagata, Y.; Oshima, R.; Maeda, Y. *J. Phys. Chem. B* **2000**, *104*, 6028.
(21) Scott, R. W. J.; Wilson, O. M.; Oh, S.; Kenik, E. A.; Crooks, R. M. *J. Am. Chem. Soc*. **2004**, *126*, 15583.
(22) Liu, H. B.; Pal, U.; Medina, A.; Maldonado, C.; Ascencio, J. A. *Phys. Rev. B* **2005**, *71*, 075403.
(23) Baletto, F.; Mottet, C.; Ferrando, R. *Phys. Rev. Lett* **2003**, *90*, 135504.
(24) Rodriguez−Gonzalez, B.; Burrows, A.; Watanabe, M.; Kiely, C.; Liz-Marzan, L. M. *Jour. Mater. Chem.* **2005**, *15*, 1755
(25) Lia, Z. Y.; Yuanb, J.; Chen, Y.; Palmer, R. E.; Wilcoxon, J. P. *Appl. Phys. Lett*. **2005**, *87*, 243103.
(26) Remita, H.; Etcheberry, A.; Belloni, J. *J. Phys. Chem. B* **2003**, *107*, 31.
(27) Fujikawa, T.; Idei, K.; Ohki, K.; Mizuguchi, H.; Usui, K. *Appl. Catal. A* **2001**, *205*, 71.
(28) Yonezawa, T.; Toshima, N. *J. Chem. Soc. Faraday Trans*. **1995**, *91*, 4111.
(29) (a) Rossi, G.; Rapallo, A.; Mottet, C.; Fortunelli, A.; Baletto, F.; Ferrando, R. *Phys. Rev. Lett.* **2004**, *93*, 105503. (b) Baletto, F.; Mottet, C.; Ferrando, R. *Phys. Rev. B* **2002**, *66*, 155420.
(30) Shirinyan, A. S.; Wautelet, M. *Nanotechnology* **2004**, *15*, 1720.
(31) Wautelet, M.; Shirinyan, A. *Archs. Metall. Mat.* **2006**, *51*, 539.
(32) Guisbiers, G.; Wautelet, M. *Nanotechnology* **2006**, *17*, 2008.

NL070694A